Viruses as a tool in nanotechnology and target for conjugated polymers

Gruszka, Agnieszka

Chapter 3 Electrical properties of carbon nanotubes insulated in biological cages

3.1 Introduction

The high demand for new generation of functional materials is the driving force for development of innovative hybrids. Particularly interesting is the interface of biology and material science where the era of bioelectronics has started[1]. To convert a biological event into a measurable electronic signal one needs to develop building blocks that communicate with each other. In the first place, these constructs need to contain either proteins or nucleic acids to ensure specificity of signal recognition. Secondly, these biopolymers need to be coupled to a material that will offer mechanical stability and, preferably, facilitate the readout of the produced signal. Here, carbon nanotubes (CNTs) with their exceptional mechanical and electronic properties seem to be a perfect candidate.

Almost immediately after their discovery in 1991, the use of Single-Walled Carbon Nanotubes (SWCNTs) as functional material has been extensively investigated[2]. SWCNTs are seamless, hollow cylinders made of graphene sheets. The diameter of SWCNT varies around 1-2 nm while their length reaches several micrometres, which qualifies them as one-dimensional objects with high aspect ratio. The CNTs can be also found as Double-Walled and Multi-Walled variants (DWCNT and MWCNT, respectively) when comprised of two or more graphene layers. Their diameters are then appropriately larger, reaching <100 nm for MWCNTs[3]. The molecular structure of all carbon nanotubes gives them

unique electronic and mechanical properties paired with an outstanding chemical stability[4]. Walls of SWCNTs are solely built of sp^2 hybridized carbon atoms that are arranged hexagonally, just as in conjugated aromatic benzene rings. This property contributes to a high in-plane rigidity of the nanotube walls and renders them chemically stable. In fact the chemical bonds forming the CNT surfaces are stronger than the ones present in diamonds. The exclusive sp^2 bonding is also the reason for the electronic structure of SWCNT, which can be seen as *giant conjugated molecular wires with the conjugation length corresponding to the whole length of the tube*[5]. However, it has to be noted that not all carbon nanotubes have the same electronic properties. As there are multiple ways how the graphene sheet can be rolled up to form a tube, the SWCNT can have either metallic or semiconducting (SC) character. The synthesis process is still not controllable and therefore SWCNTs are always obtained as a mixture. Despite the necessity of cumbersome purification to obtain materials of defined electrical properties, much attention has been focussed on the isolation of semiconducting carbon nanotubes[6-8].

Although it might seem that the ultimately hydrophobic CNTs are not compatible with water-soluble biomacromolecules, both DNA and proteins are known to interact with their surface. The binding of polypeptides to the CNTs is mainly unspecific[9]. It is driven by weak van der Waals forces, hydrophobic interactions, and π-π stacking. Besides, it always involves protein's hydrophobic domains, which can lead to comprised protein functionality. To circumvent this, specific binding strategies were introduced including linkers covalently bound to the CNT surface. Although the function of the protein is ensured, this approach might impair the electric properties of the tube. At the same time, the diverse unspecific interactions may lead to fouling of the nanotube surface by adsorption of other molecules or proteins. To overcome these problems addition of polymers or surfactants to wrap the CNTs was suggested[10]. Nevertheless, the strategies of controlled coupling of proteins with CNTs are still far from satisfactory. In contrast, DNA interacts more specifically with CNTs. The helical structure of nucleic acids is perfectly suitable for this purpose because hydrophobic nucleobases coordinate to the carbon surface while the phosphate backbone ensures solubility in water[11]. It was shown that basically any DNA sequence can solubilize CNTs in water, mostly yielding monodisperse SWCNTs[12]. Several specific sequences have been selected

to isolate SWCNTs regarding their chirality and hence electronic properties[11,13,14]. Additionally, the DNA binding to the CNT surface is strong enough to enable chromatographic separation[14]. Thus, DNA can greatly facilitate not only separation of the single chirality SWCNTs, but also their purification by automated methods. Aside from that, the functionality of oligonucleotides is retained, which leaves an opportunity to use them for detection purposes or to control self-assembly[15,16].

Up to now both proteins and DNA have been successfully integrated in CNT-based nanoscale electronic devices. Such devices work either as electrochemical sensors or field effect transistors. In electrochemical devices, the CNTs replaced traditional carbon electrodes. These sensors are widely used to detect neurotransmitters and benefit from i.a. enhanced adsorption of analytes, better electrocatalytical activity and rapid electrode kinetics[17].

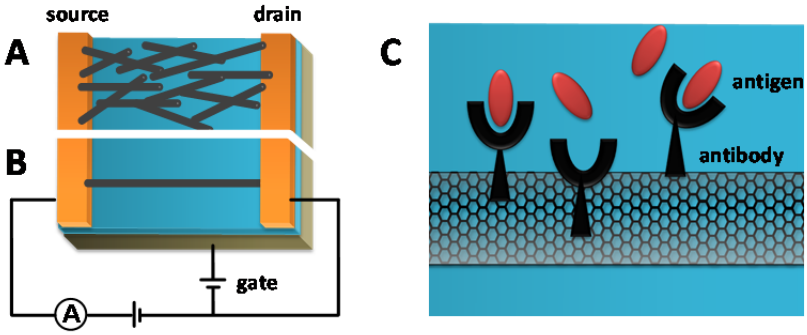

Figure 3.1. Schematic representation of CNT-FET device assembled with a CNT network (A) or with a single tube (B). Working principle of bioactive CNT-FET (C).

In field effect transistor based sensors, SWCNTs are used as a conducting material (Figure 3.1). A typical FET is a three electrode device where the current flows through a semiconductor channel, which is positioned between source and drain electrodes, and separated from the third electrode (gate) by a layer of insulator. The current applied to the gate influences the charge carriers in the semiconductor and, therefore, the conductance of the channel is modulated by the gate voltage. Thus the device on/off state is controlled by the voltage applied to the gate.

In principle, any change in the local environment of the semiconductor will influence its conductance in a similar manner as the gate voltage does. These changes can be for example caused by fluctuations in number of CNT-bound DNA strands due to DNA hybridisation, antibody binding or an enzymatic reaction. All these events will likely introduce a local charge variation and a consequential rearrangement of the ionic species at the surface of the very sensitive semiconducting channel. Hence, this recognition event can be further translated into a sensor response[18].

The first field effect biosensor based on carbon nanotubes (CNT-FET) was described in 2003. It was a pH sensor built with a single SWCNT, which was modified with a redox enzyme, glucose oxidase[19]. Soon after, well-established biological components were implemented in the CNT-FET sensors. For example binding of streptavidin to the biotinylated surface of SWCNTs[20] and detection of human antigens with SWCNT devices modified with a specific antibody were measured[1]. The DNA hybridization is a second attractive mode of action that has been realized with CNT-FETs[16]. Such devices can specifically recognize target DNA strands with up to picomolar limit of detection, and also differentiate between single base mismatched sequences. Besides, the sensitivity of a SWCNT transistor with covalently attached ssDNA has been even utilized to study kinetics and thermodynamics of DNA hybridization events[21]. Furthermore, a range of CNT-FET biosensors for detection of small, biologically relevant molecules, such as cholesterol, glucose, nitrite oxide or dopamine has been constructed. This field is likely going to expand due to rapid progress in development of aptamers[22]. Last but not least DNA oligonucleotides are very useful for the controlled assembly of SWNT FETs of different architectures[15,16,23].

In this chapter we aim to probe electric properties of SWCNTs encapsulated by a protein shell of viral origin. At first, a method to purify monodispersed semiconducting SWCNTs will be described. Afterwards, the SWCNTs will be encapsulated in a protein cage employing Cowpea Chlorotic Mottle Virus coat proteins (CCMV CPs). Finally the electrical properties of the Virus-like Carbon Nanotube (VL-CNT) will be evaluated in two types of field effect transistors. The measurements of the single tube device will be performed with the help of atomic force microscopy operating in conducting mode. Subsequently, a device based on a VL-CNT network will be constructed and evaluated.

3.2 Results and discussion

3.2.1 Preparation of semiconducting carbon nanotubes

The purity of CNTs defines their functioning as a building block in electronic devices. Therefore, it was necessary to obtain SWCNT dispersion, which almost exclusively contains semiconducting species for incorporation into CNT-FETs. At first, commercially available SWCNTs enriched with (6.5) species were employed. They were dispersed with 22-mer DNA sequence, which efficiently templated VL-CNT formation as described in section 2.2.4. Unfortunately the fraction of metallic CNTs still present in the solution was too high to construct a functional FET device despite semiconducting species-enriched starting material. Therefore, in the next step we have employed a 12-mer oligonucleotide $(TAT)_4$ that proved to efficiently separate semiconducting (6.5) species[13].

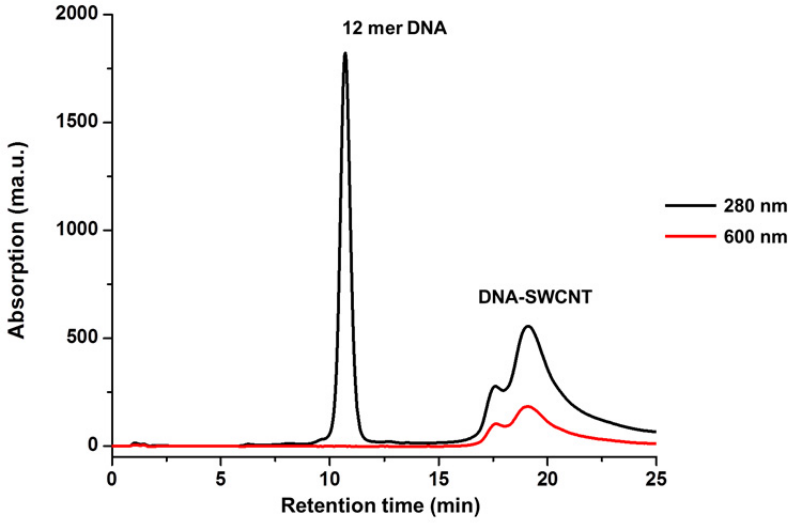

Figure 3.2. HPLC purification of (6.5) tubes.

The SWCNT dispersion was prepared with the help of a sonication bath in a straightforward experiment as described in section 2.2.1. However the isolation of monodispersed semiconducting species proceeded in different manner. After the centrifugation step, the SWCNT solution was purified on a strong anion-exchange (AEX) column. A chromatographic

separation of DNA-dispersed SWCNT is presented in Figure 3.2. The purification was simultaneously monitored at two wavelengths. The wavelength of 280 nm was chosen as DNA-specific, whereas 600 nm indicated the elution of SWCNT. The absorption maxima of semiconducting species fall in the range of 950-1500 nm, however, they could not be used due to hardware limitations. Nonetheless, 600 nm offers sufficient level of sensitivity for purification purposes due to an overlap with a second absorption maximum of semiconducting CNTs. The first eluting peak (retention time 11 min) corresponds to pristine DNA present in dispersing buffer whereas the second peak with a longer retention time contains the hybrid material as verified by dual-absorption. The stronger interaction of the DNA-SWCNTs with the anion-exchange resin is a consequence of multiple DNA strands tightly wrapping the SWCNT surface. Fractions of 200 μL were collected during the elution (16-20 min) and afterwards they were manually analysed with a spectrophotometer in order to isolate pure semiconducting species. The (6.5) SWCNT eluted in early fractions (16-17.5 min). These solutions were combined, desalted, and stored in the 100 mM NaCl, which resembles the salt composition of the buffer used to prepare dispersions.

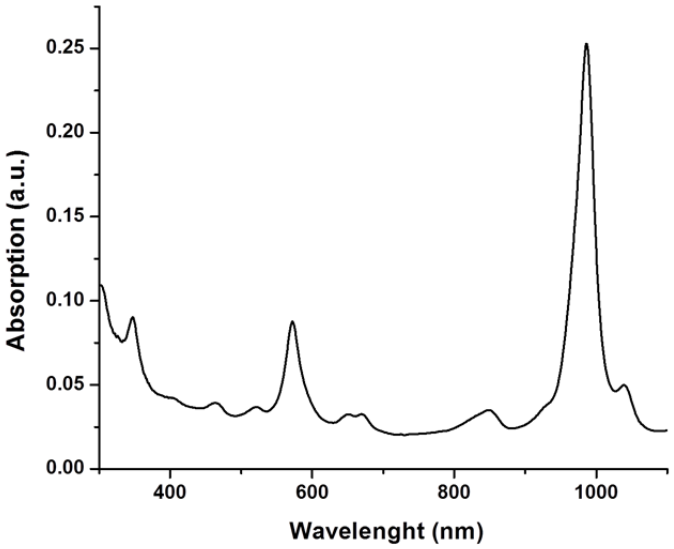

Figure 3.3. Absorption spectrum of AEX purified (6.5) SWCNTs.

The absorption spectrum of the purified SC species is shown in Figure 3.3. E_{11} and E_{22} absorption maxima (986 nm and 572 nm) correspond to the values reported for (6.5) SWCNTs (988 nm and 571 nm, respectively)[13]. The small peak at 1039 nm corresponds to the presence of 7.5 semiconducting species, which have slightly wider diameter and therefore were enriched in the succeeding fractions[13]. The yield of purification was estimated to be 0.23% due to significant and irreversible binding of the carbon nanotube material to the AEX column. The quality of dispersion was sufficient for incorporation in the CNTs-protein hybrid and subsequent evaluation in a FET set up.

3.2.2 Assembly of virus-like carbon nanotube

To date, application of plant virus coat protein (CP) was found to yield unprecedented coverage of the CNT surface, which was described in Chapter 2. Thus the SWCNTs dispersion obtained with $(TAT)_4$ sequence was considered to be compatible with the previously described strategy based on Cowpea Chlorotic Mottle Virus (CCMV) CP.

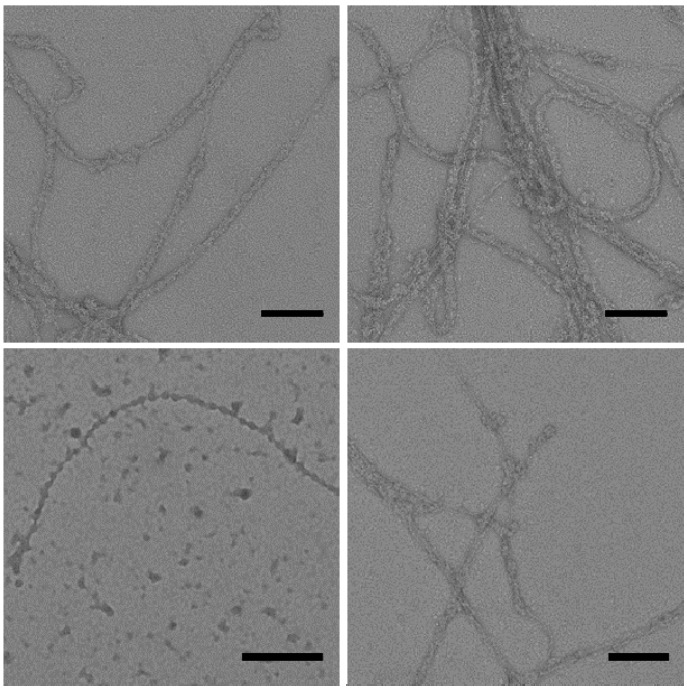

Figure 3.4. Encapsulation of SWCNTs dispersed with 12-mer DNA sequence. Scale bars 100 nm.

In short, the (6.5) SWCNTs solution was incubated with CCMV CP overnight at 4°C in neutral pH. Subsequently the quality of the protein coating was controlled with transmission electron microscopy (TEM). Unexpectedly, it was revealed that dispersion obtained with 12-mer didn't template a proper VLP formation. The protein layer was partial and not uniform as visible in Figure 3.4. We assumed that it might be associated to a reduced length of the oligonucleotide used in the dispersion when compared to the previously conducted experiments. Therefore, in the next step we supplemented the $(TAT)_4$–CNT dispersion with 22-mer sequence and subjected it to additional round of sonication. We anticipated that the longer sequence would additionally get adsorbed on the CNT surface or would replace some of the short DNA strands originally used.

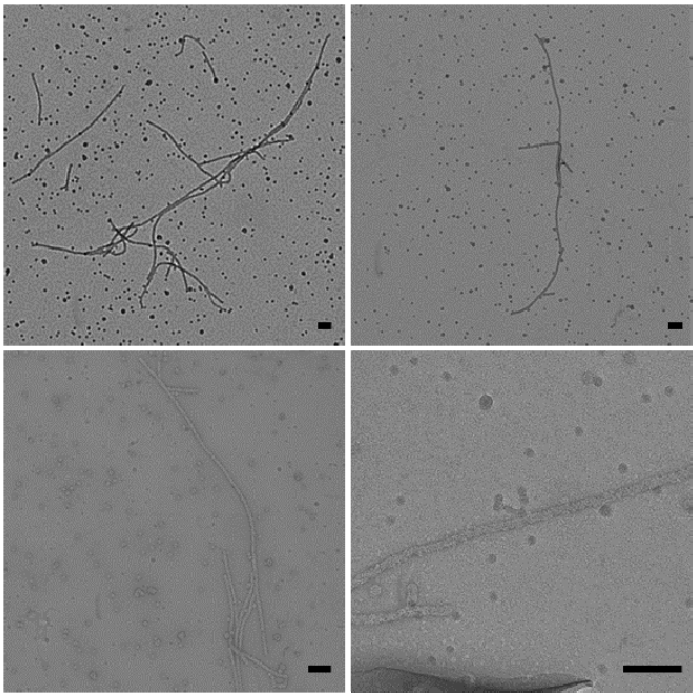

Figure 3.5. Encapsulation of SWCNTs dispersed with 22-mer DNA sequence. Scale bars 100 nm.

In fact, the addition of 22-mer to the dispersing buffer greatly improved the coverage of the SWCNTs surface (Figure 3.5). The formed VL-CNTs exhibited uniform protein shell of 22-23 nm diameter as it was observed before (Chapter 2). However it remains uncertain why SWCNTs

dispersed with 12-mer did not efficiently induced virus-like particle formation. It is known that a certain charge density on the template molecule is necessary to attract multiple CPs and nucleate capsid formation[24]. However, we expected that this condition was fulfilled by 12-mer compactly wrapping a SWCNT around, as concluded from computational simulations[25]. Hence we assume that a very local charge density is crucial here. Secondly, the binding strength of nucleobases to the surface of SWCNTs is not the same. Guanine and cytosine bind stronger than adenine and thymine bases[26]. The 22-mer is GC rich molecule which might provide more a robust scaffold for the CCMV CP assembly than $(TAT)_4$.

3.2.3 Single tube FET device measurement

To study the electrical properties of the protein-coated CNTs atomic force microscopy (AFM) working in conducting mode (c-AFM) was employed. This is a powerful microscopy technique, which enables not only high resolution mapping of the specimen active surface, but also facilitates electrical characterisation of a single nano-object.

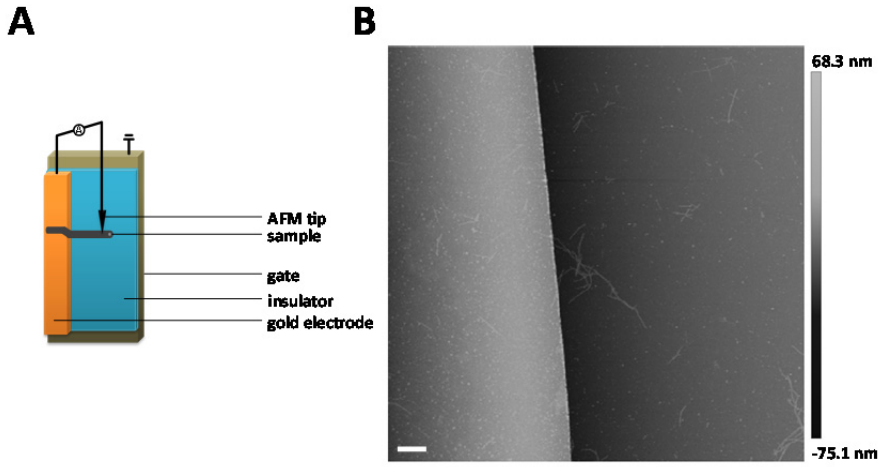

Figure 3.6. Scheme of single molecule FET for c-AFM experimental set up (A). AFM image of the measured device recorded in the tapping mode. Scale bar corresponds to 1 µm (B).

The scheme of a FET device incorporating the protein coated SWCNTs studied with c-AFM is presented in Figure 3.6A. In short, the CNT works

as a semiconducting channel bridging a gold electrode (source) and an AFM probe (drain). Current flowing through the probe (I_{S-D}) can be recorded because the AFM tip utilized for c-AFM is coated with metal (or metal alloy). If the channel material shows semiconducting properties, its conductivity can be regulated by gate voltage.

At first, AFM was employed in tapping mode to localize a VL-CNT, which bridges the gold electrode with the non-active area of the substrate (Figure 3.6B). Afterwards, the c-AFM probe was placed on the protein-wrapped CNT and current flowing through it was recorded.

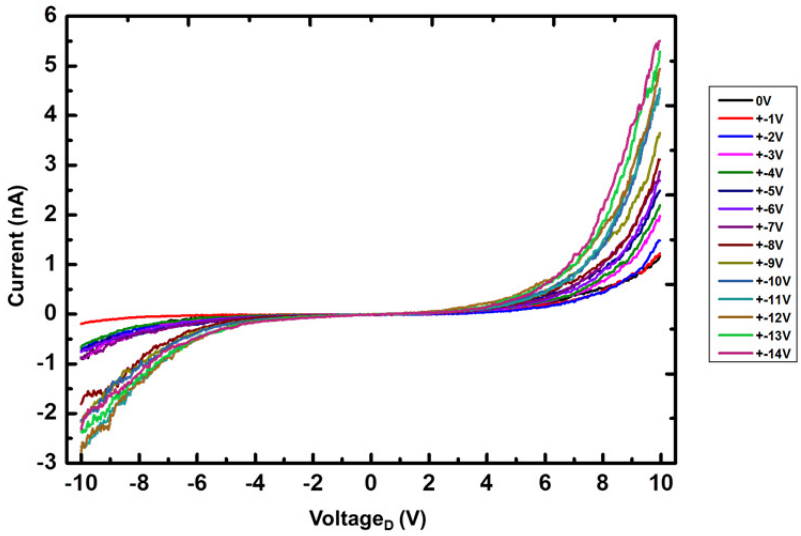

Figure 3.7. Characterization of the single CNT-FET with c-AFM.

The FET characteristic curves are presented in Figure 3.7. The gate voltage was modulated in 1 V steps from 0 to 14 V and from 0 to -14 V to record positive and negative I_{S-D} current, respectively. The device showed gate-regulated I_{S-D} for both negative and positive gate voltages, which suggested its ambipolar behaviour. The measured current was in nanoamper range which is 10^2-10^3 times lower than values previously reported for single SWCNT transistors[15,27].

In order to be able to directly compare the effect of protein layer on the channel conductivity, we performed an experiment where DNA dispersed tubes were also included.

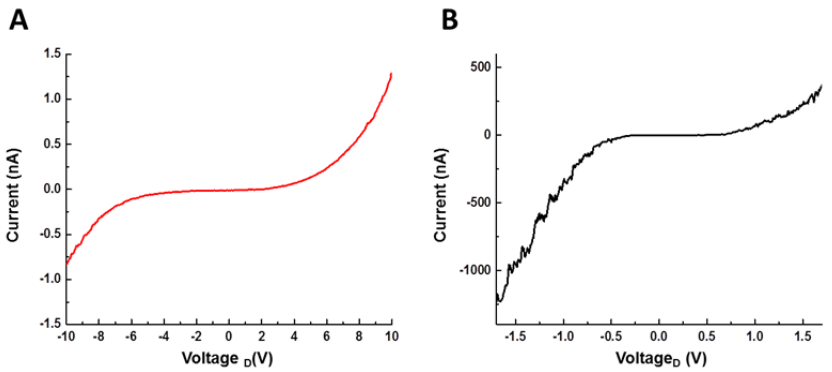

Figure 3.8. Comparison of I-V characteristics of the FET devices assembled with protein-coated (A) and uncoated (B) semiconducting SWCNTs.

To this end, two devices with the same architecture were fabricated in parallel and the I-V curves for VL-CNT and DNA-dispersed CNT devices were recorded at the same gate voltage (±1.5 V). We anticipated that biomacromolecules hierarchically assembled on the CNT would exhibit insulating behaviour. In fact, the current measured for protein wrapped CNT FET was over thousand times lower than for uncoated CNT as shown in Figure 3.8 (for V_D=-1.5 V).

This strong electrical insulation represents an elegant way to prove that the virus protein formed a closed structure around the SWCNT.

3.2.4 Measurement of protein-coated SWCNT networks in a macroscopic devices.

Electrical devices built from a single CNT are important tool to study the SWCNT regarding the electrical properties. However, integration of a single tube in an electrical circuit is extremely cumbersome from a technological point of view. Additionally, any variations in chirality and diameter of the applied material can potentially lead to changing results in future up-scaled applications. Therefore, after having assessed the electrical properties of the semiconducting VL-CNTs on the single tube level, we aimed to test performance of this new biohybrid material in a macroscopic device. Such devices are fabricated with the CNT network and they offer faster measurements and do not require c-AFM.

The active layer in the FET device was formed by drop casting of the VL-CNT aqueous solution on the substrate surface. In order to remove

excess of salts present in the protein assembly buffer, the substrate was additionally washed with ultrapure water. Subsequently, I-V curves were recorded for positive and negative gate voltages.

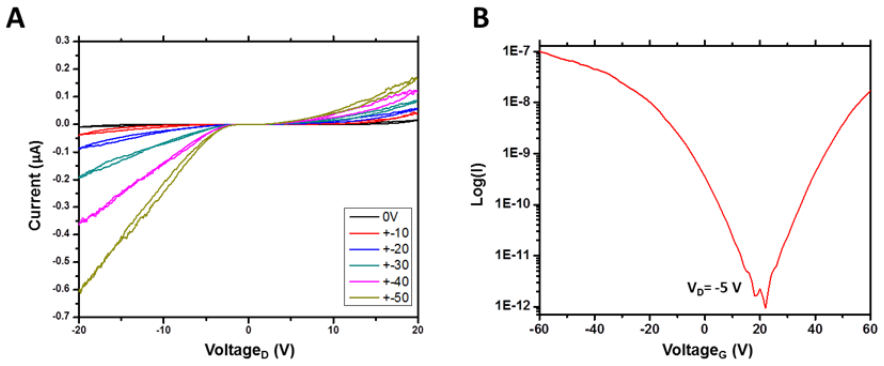

Figure 3.9. I-V characteristics of device assembled with VL-CNT network (A). I-V characteristics of the VL-CNT device from which on/off ratio was extracted (B)

As expected after single tube measurements, the network device also exhibited FET characteristics. However, the recorded $I_{S\text{-}D}$ current of the protein-coated SWCNT network was three orders of magnitude higher than $I_{S\text{-}D}$ measured for a single protein-coated tube (Figure 3.9A). This may be the result of multiple contacts with electrodes within the device. Again, the insulating properties of protein shell were confirmed (Supporting Figure 3.1). Next, the I-V curves presented in Figure 3.9B were used to calculate on/off ratio of the VL-CNT FET. This parameter describes the potential of application in electronic circuits for sensors or memory storage. The calculated on/off ratio reaches 10^4-10^5, which is remarkably high when compared to state of the art CNT FETs built with polymer-isolated semiconducting species (10^8)[28]. Additionally, we anticipate that the presence of insulating protein layer can significantly reduce the influence of metallic contaminants in the measured network.

3.3 Conclusion

In this chapter, we described a method to obtain individually dispersed semiconducting carbon nanotubes encapsulated in an insulating protein shell. Secondly we implemented such hybrids in functional field effect devices and assessed their electrical properties on the single tube level as well as in a tube network.

The SWCNTs exhibiting (6.5) chirality were dispersed in water with the help of a specific DNA sequence and were afterwards purified using an automated HPLC method. The dispersion was used as a template for assembly of plant virus coat proteins around single SWCNTs. Here, it was revealed that the length of the oligonucleotide employed to form the dispersion greatly influences the protein shell formation. Subsequently, the new hybrid material was used to build two types of field effect transistors (FET). The single tube FET device was used to evaluate the impact of protein shell on the electronic properties of the SWCNT. As anticipated, virus coat protein caused significant level of electrical insulation because the measured conductivity dropped by three orders of magnitude when compared to DNA-dispersed CNTs. These experiments clearly indicated that the virus shell formed by CCMV CP is a closed system. Despite obvious contact resistance caused by two layers of biological macromolecules, the I-V curves revealed semiconducting properties of the constructed virus-like carbon nanotubes (VL-CNTs). It indicated that the SWCNT's functionality is preserved in the hybrid. In the next step, the VL-CNTs network-based FETs were investigated. The device exhibited comparable FET behaviour, however, as expected the measured current was higher due to the multiple contacts of SWCNTs with the electrodes and multiple conducting pathways. Additionally, the protein shell may improve the overall performance of the VL-CNT device because it is able to largely insulate any metallic species remaining in the dispersion. The characteristic I-V curves of the device were used to determine on/off ratio of VL-CNT FET, which was 10^4-10^5.

Finally, we believe that presented CNT-protein hybrid brings new opportunities in the field of SWCNT-based biosensors. It overcomes the need of CNT's surface passivation which is often advised to prevent nonspecific adsorption in complex biological samples. At the same time the surface of the protein coating is available for modification with a target-sensitive unit.

3.4 Materials and methods

All chemicals were purchased from commercial sources (Sigma Aldrich, Acros Organics) and used as received without further purification. Single Walled Carbon Nanotubes enriched with (6.5) species were obtained from Sigma Aldrich. The DNA oligomers (5'-CCT CGC TCT GCT AAT CCT GTT A-3' and 5'-TAT TAT TAT TAT-3') were obtained from

Biomers (Ulm, Germany) at HPLC purity grade. Copper grids (400 mesh) were purchased from Science Services (Germany). The sonication bath (VWR, The Netherlands, 150 W) was operated at 45 kHz. Centrifugal dialysis devices (Vivaspin 500 MWCO 50 kDa, Sartorius Stedim), dialysis membranes (RC, 6 Spectra/Por, Spectrum® Laboratories) and anion exchange column (Hi Trap Q, GE Healthcare) were obtained from VWR. In all experiments, ultrapure water with a resistivity of 18.2 MΩ/cm was used. Absorption spectra were recorded on a UV-Vis spectrophotometer (Jasco V-630). Atomic Force Microscopy characterization was performed using a MultiMode 8 AFM Microscope with System Controller V.

CCMV was provided by Prof. Dr. J.J.L.M. Cornelissen (MESA+ Institute, University of Twente, Enschede, The Netherlands).

Dispersion and purification of (6.5) SWCNT

The SWNT dispersion was prepared according to protocols reported elsewhere with modifications[11,14]. In short, a sample of (6.5) enriched SWCNT was weighted into a glass vial and placed in the ice-cold sonication batch. A dispersing buffer (1 mg/mL of DNA in 0.1 M NaCl) at a total volume of 100 µL/100 µg of SWCNTs was added in 5 equal portions every 30 min. Dispersed SWCNTs were centrifuged for 1 hour in a bench-top centrifuge (16k rpm) to remove insoluble material and afterwards purified on HPLC (AKTA Explorer). The following mobile phases were employed: 20 mM 2-(N-morpholino)ethanesulfonic acid (MES) as mobile phase A and 1.8M NaSCN in 20 mM MES as buffer B. Purification was performed on HiTrap Q HP 1 mL column (GE Healthcare) using a linear gradient of buffer B and monitored using wavelengths of 280 nm and 600 nm. Fractions of 200 µL were collected and their absorption spectra were measured to identify the ones containing (6.5) SWCNTs. Selected fractions were combined, concentrated and washed with 0.1M NaCl buffer using Vivaspin centrifugal devices (50k MWCO, GE Healthcare).

Next, 500 µL dispersion was supplemented with 22-mer to the final concentration of 1 mg/mL and sonicated in the ice batch for additional 30 min. To remove excess of DNA, the dispersion was washed twice with 0.1 M NaCl using another Vivaspin centrifugal device as described above and finally concentrated to 200 µL of solution $OD_{986\ nm}$=0.8 (8 µg/mL).

Coating with CCMV capsid protein
The virus capsid solution was dialyzed overnight against (300 mM NaCl, 50 mM Tris, 1mM EDTA, 10 mM $MgCl_2$, pH=7.4). Afterwards, protein concentration was determined by measuring absorption at 280 nm (ε=24.075 $M^{-1}cm^{-1}$) to be 3.3 mg/mL. Carbon nanotube concentration was adjusted to 6 μg/mL with buffer used for dialysis. Afterwards they were mixed with CP solution in 1:50 ratio (w/w) and incubated overnight at 4°C. The quality of the resulting coating was determined with TEM.

Transmission Electron Microscopy
The TEM samples were prepared by depositing 5 μL of sample (diluted in ultrapure water) on a glow-discharged carbon-coated copper grid (400 mesh). After 10 sec, the excess of liquid was blotted on a paper filter. The sample was washed once with ultrapure water to remove salts. The samples were negatively stained with uranyl acetate by depositing 5 μL of the stain solution for 10 seconds and blotting the excess on a paper filter (repeated twice). Pictures were collected on a Philips CM120 transmission electron microscope operated at 120 kV in the bright field mode.

c-AFM
The sample was deposited on the surface of the substrate and incubated for 5 minutes at 100% humidity to facilitate adsorption of the CNTs to the surface. Afterwards, the excess of the liquid was removed by blotting off on a filter paper. The substrate was washed 3 times with ultrapure water to remove salts and dried at room temperature under argon atmosphere.

The height images of protein-coated SWNTs were measured in tapping mode with a TESP-V2 probe. Subsequently, TUNA extended mode was used for the current recording in contact mode under ambient conditions. ANSCM-PC probes with a spring constant of k = 0.2 N/m, tip radius 30 nm and tip height 2.5-8 μm were utilized. The scanning region was selected with a size of up to 70 μm by 70 μm. The scanning rate and number of lines were selected to be 0.2 Hz and 1024-2048 lines/sample, respectively.

Macroscopic devices
The active layer was formed by drop casting of the VL-CNT sample. Solution was deposited on the surface of a commercial Si/SiO2

substrates pre-patterned with an interdigitated Ti/Au structure with a channel length of 10 µm and a channel width of 10 mm. The substrate was incubated for 5 minutes in 100% humidity to facilitate adsorption of the CNTs to the surface. Afterwards, the excess of the liquid was removed by blotting off on a filter paper. The substrate was washed 3 times with ultrapure water to remove salts and dried at room temperature under argon atmosphere and stored in nitrogen-filled glove box prior measurement to remove the absorbed oxygen. The electrical measurements were performed with a semiconductor parameter analyser (Agilent E5262A) in a nitrogen-filled glove box.

3.5 Supporting information

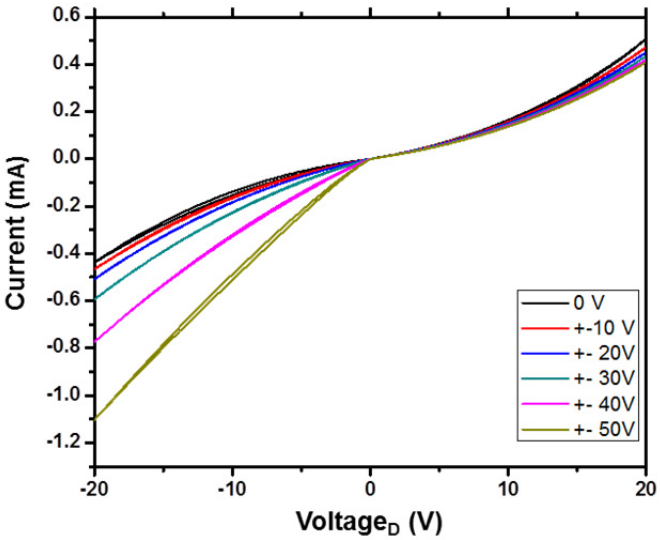

Supporting Figure 3.1. I-V characteristics of device assembled with DNA-CNT network. The measured current is in miliamper range, which is 10^3 higher than I_{S-D} of VL-CNT device.

3.6 Acknowledgment

I would like to acknowledge V. Derensky for performing macroscopic device measurements and Dr. P. Gordiichuk for performing AFM measurements.

3.7 References

1. Zhang, A. & Lieber, C.M. Nano-Bioelectronics. *Chem Rev* **116**, 215-257 (2016).
2. Iijima, S. Helical microtubules of graphitic carbon. *Nature* **354**, 56-58 (1991).
3. Baughman, R.H., Zakhidov, A.A. & de Heer, W.A. Carbon nanotubes-the route toward applications. *Science* **297**, 787-792 (2002).
4. Dai, H. Carbon nanotubes: synthesis, integration, and properties. *Acc Chem Res* **35**, 1035-1044 (2002).
5. Forró, L. & Schönenberger, C. Carbon nanotubes, materials for the future. *Europhysics News* **32**, 86-90 (2001).
6. Gao, J., Kwak, M., Wildeman, J., Herrmann, A. & Loi, M.A. Effectiveness of sorting single-walled carbon nanotubes by diameter using polyfluorene derivatives. *Carbon* **49**, 333-338 (2011).
7. Gomulya, W.*, et al.* Semiconducting single-walled carbon nanotubes on demand by polymer wrapping. *Adv Mater* **25**, 2948-2956 (2013).
8. Samanta, S.K.*, et al.* Conjugated polymer-assisted dispersion of single-wall carbon nanotubes: the power of polymer wrapping. *Acc Chem Res* **47**, 2446-2456 (2014).
9. Calvaresi, M. & Zerbetto, F. The Devil and Holy Water: Protein and Carbon Nanotube Hybrids. *Acc Chem Res* **46**, 2454-2463 (2013).
10. Allen, B.L., Kichambare, P.D. & Star, A. Carbon Nanotube Field-Effect-Transistor-Based Biosensors. *Adv Mater* **19**, 1439-1451 (2007).
11. Zheng, M.*, et al.* DNA-assisted dispersion and separation of carbon nanotubes. *Nat Mater* **2**, 338-342 (2003).
12. Umemura, K. Hybrids of Nucleic Acids and Carbon Nanotubes for Nanobiotechnology. *Nanomaterials* **5**, 321 (2015).
13. Tu, X., Manohar, S., Jagota, A. & Zheng, M. DNA sequence motifs for structure-specific recognition and separation of carbon nanotubes. *Nature* **460**, 250-253 (2009).
14. Zheng, M.*, et al.* Structure-based carbon nanotube sorting by sequence-dependent DNA assembly. *Science* **302**, 1545-1548 (2003).
15. Hazani, M.*, et al.* DNA-mediated self-assembly of carbon nanotube-based electronic devices. *Chem Phys Lett* **391**, 389-392 (2004).
16. Jung, S.*, et al.* Dissociation of single-strand DNA: single-walled carbon nanotube hybrids by Watson-Crick base-pairing. *J Am Chem Soc* **132**, 10964-10966 (2010).
17. Jacobs, C.B., Peairs, M.J. & Venton, B.J. Review: Carbon nanotube based electrochemical sensors for biomolecules. *Anal Chim Acta* **662**, 105-127 (2010).
18. Veigas, B., Fortunato, E. & Baptista, P.V. Field effect sensors for nucleic Acid detection: recent advances and future perspectives. *Sensors* **15**, 10380-10398 (2015).

19. Besteman, K., Lee, J.-O., Wiertz, F.G.M., Heering, H.A. & Dekker, C. Enzyme-Coated Carbon Nanotubes as Single-Molecule Biosensors. *Nano Lett* **3**, 727-730 (2003).
20. Star, A., Gabriel, J.-C.P., Bradley, K. & Grüner, G. Electronic Detection of Specific Protein Binding Using Nanotube FET Devices. *Nano Lett* **3**, 459-463 (2003).
21. Sorgenfrei, S.*, et al.* Label-free single-molecule detection of DNA-hybridization kinetics with a carbon nanotube field-effect transistor. *Nat Nanotechnol* **6**, 126-132 (2011).
22. So, H.-M.*, et al.* Single-Walled Carbon Nanotube Biosensors Using Aptamers as Molecular Recognition Elements. *J Am Chem So* **127**, 11906-11907 (2005).
23. Kwak, M.*, et al.* DNA block copolymer doing it all: from selection to self-assembly of semiconducting carbon nanotubes. *Angew Chem Int Ed Engl* **50**, 3206-3210 (2011).
24. Cadena-Nava, R.D.*, et al.* Self-assembly of viral capsid protein and RNA molecules of different sizes: requirement for a specific high protein/RNA mass ratio. *J Virol* **86**, 3318-3326 (2012).
25. Roxbury, D., Jagota, A. & Mittal, J. Structural characteristics of oligomeric DNA strands adsorbed onto single-walled carbon nanotubes. *J Phys Chem B* **117**, 132-140 (2013).
26. Albertorio, F., Hughes, M.E., Golovchenko, J.A. & Branton, D. Base dependent DNA-carbon nanotube interactions: activation enthalpies and assembly-disassembly control. *Nanotechnology* **20**, 395101 (2009).
27. Keren, K., Berman, R.S., Buchstab, E., Sivan, U. & Braun, E. DNA-templated carbon nanotube field-effect transistor. *Science* **302**, 1380-1382 (2003).
28. Derenskyi, V.*, et al.* Carbon nanotube network ambipolar field-effect transistors with 10(8) on/off ratio. *Adv Mater* **26**, 5969-5975 (2014).